Journal of Building Engineering 103 (2025) 112058

Contents lists available at ScienceDirect

Journal of Building Engineering

journal homepage: www.elsevier.com/locate/jobe

Analysis of thermal performance of an innovative thermal storage wall

Cansu Bekler [a], İdil Ayçam [a], Mustafa Zeki Yılmazoğlu [b,*]

[a] Department of Architecture, Faculty of Architecture, Gazi University, Ankara, Türkiye
[b] Department of Mechanical Engineering, Faculty of Engineering, Gazi University, Ankara, Türkiye

ARTICLE INFO

Keywords:
Transparent insulation
Phase change material
Energy storage
Energy efficiency

ABSTRACT

This study examines the thermal performance and impact on thermal comfort of an innovative wall combining Transparent Insulation Material (TIM), Phase Change Material (PCM), and an Air Gap (AG) to reduce building energy consumption. The wall boosts solar energy gains through TIM, prevents PCM overheating with AG, and utilizes PCM-integrated bricks as thermal mass. Using Ankara's climate data, its performance during heating (January, 21) and cooling (July, 21) was analyzed via numerical and dynamic simulations, focusing on heat transfer (Q), Decrement Factor (DF), and Time Lag (TL). MATLAB analysis of five organic PCMs with different melting points identified RT18HC for heating and RT22HC for cooling. The TIM-AG-PCM wall delayed temperature transmission by 8.33 h in heating and 4.38 h in cooling, with an amplitude reduction of 0.24. Dynamic simulation in HTflux showed a time shift difference of 33 min for heating and 28 min for cooling compared to MATLAB results, with DF and Q values showing 70 % and 95 % similarity, respectively. Mean Radiant Temperature (MRT) analysis in a virtual room demonstrated the wall's ability to reduce indoor temperature fluctuations and maintain conditions near thermal comfort. The conclusions confirm that the TIM-AG-PCM wall significantly improves thermal performance and contributes to energy efficiency in buildings.

Nomenclature

T	Temperature [°C]
T_{pcm}	PCM temperature [°C]
T_m	Melting temperature of PCM [°C]
$T_{e,wall}(t)$	Wall external surface temperature [°C]
$T_{i,wall}(t)$	Wall internal surface temperature [°C]
$T_{i,wall}^{max}$	Maximum internal wall surface temperature
$T_{i,wall}^{min}$	Minimum internal wall surface temperature
$T_{e,wall}^{max}$	Maximum external wall surface temperature
$T_{e,wall}^{min}$	Minimum external wall surface temperature

Greek letters

λ	Thermal conductivity [W/m.K]
h	Heat transfer coefficient [W/m^2.K]
h_i	Internal heat transfer coefficient by convection [W/m^2.K]
h_o	External heat transfer coefficient by convection [W/m^2.K]
ε	Emissivity
σ	Stefan-Boltzmann constant [W/m^2.K^4]
ρ	Density [kg/m^3]
α_G	Absorbtivity
ΔT	Phase change transition temperature [°C]

(*continued on next page*)

* Corresponding author.
E-mail address: zekiyilmazoglu@gazi.edu.tr (M.Z. Yılmazoğlu).

https://doi.org/10.1016/j.jobe.2025.112058
Received 1 December 2024; Received in revised form 14 January 2025; Accepted 6 February 2025
Available online 8 February 2025
2352-7102/© 2025 Elsevier Ltd. All rights are reserved, including those for text and data mining, AI training, and similar technologies.

(*continued*)

Nomenclature			
$T_d(t)$	Changing outside air temperature throughout the day [°C]	α	Heat diffusion coefficient [m^2/s]
T_{room}	Room temperature [°C]	Δx	Spacial step
T_{air}	Outdoor air temperature [°C]		
f(t)	The proportion of liquid in the material at the time of phase change		
t	Time [s]		
Q	Heat transfer rate [W]		
L_H	Latent heat [kJ/kg]		
C_p	Specific heat capacity [J/kg.K]		
I	Solar radiation [W/m^2]		
E_s	Energy savings [Wh/m^2.day]		
E	Total amount of energy [Wh/m^2.day]		
E_{wall}	Total energy per day passing through the wall without phase change material [Wh/m^2.day]		
E_{pcm}	Total amount of energy per day passing through the wall containing PCM [Wh/m^2.day]		
DF, *f*	Decrement Factor		
TL,Φ	Time Lag		
T_{cl}	Surface temperature of the clothed body		
T_r	Radiant temperature		
$F_{cl\text{-}n}$	Radiation shape factor from the body to the nth surrounding surface		
T_{db}	Dry bulb temperature [°C]		
T_{surf}	Surface temperature [°C]		
TIM	Transparent insulation material		
PCM	Phase change material		
AG	Air gap		
CFL	Courant-Friedrichs-Lewy		

1. Introduction

The increase in energy demand worldwide and the use of fossil fuels in recent years have caused an increase in greenhouse gas emissions. Global warming, climate change effects, energy crises, and environmental problems pose a danger to the world due to this. Reducing fossil-based energy consumption and meeting the demand for renewable energy sources is the method to prevent environmental disasters from occurring.

According to a study conducted among the countries of the International Energy Agency (IEA), buildings, one of the most energy-consuming sources, consume 55 % of the total electricity used, 30 % of natural gas, and are responsible for 38 % of the greenhouse gases generated [1,2]. Heating and cooling needs account for 35 % of world energy consumption in the building sector [2,3]. Approximately 60–80 % of buildings' total heat loss is heat loss in the building envelope. This reveals how important it is to improve the thermal performance of the building envelope, especially the outer wall, in terms of energy efficiency [4–6].

Passive solar technologies are capable of reducing energy consumption and increasing the number of near-zero-energy and zero-energy buildings in building envelopes. The thermal performance of buildings using the application can be significantly affected by the optical and thermophysical properties of the materials used in the exterior wall. The material's optical and thermophysical properties are the factors that determine how much heat is gained and lost from the outer wall unit area, which is affected by outdoor temperature and solar radiation. Another parameter to be considered in heat storage works where the passive method is used on the outer walls is to prevent heat losses from the wall surface to the outside. Opaque insulation materials applied to the internal or external surface of the outer wall prevent heat transfer between the indoor and the outdoor environment, but the sun cannot benefit from the passive method. Inorganic materials such as glass wool, rock wool, and synthetic-organic foams have environmental impacts, are not recyclable, and generally use primary energy sources in their production, which has increased studies on innovative materials in sustainable and energy-efficient architecture [7–11]. In this context, TIM is one of the innovative materials that should be examined in minimizing heat losses in the building envelope depending on their physical properties and ensuring that the wall works as a thermal mass by transmitting sun rays to the wall in front of the wall applications.

Using thermal storage is another way to decrease energy consumption in buildings. PCM, which can store thermal energy as latent heat, is recognized by researchers and practitioners as a promising method for integrating it into the exterior walls of buildings [12–20]. PCM's higher heat storage capacity per unit volume makes it stand out from conventional building materials. The material undergoes a phase change when the ambient temperature changes. The process of phase change is endothermic, and it absorbs heat from the environment. As the ambient temperature decreases, the PCM solidifies and releases heat into the environment. The indoor temperature fluctuations and heating and cooling loads are minimized by this cycle [21–24]. The application of PCM on the exterior wall reduces heating and cooling peak loads, improves indoor thermal comfort conditions, and ensures efficient use of passive heating and cooling loads [15,21,25–27].

It is crucial that materials science developments contribute to the strategies designed to enhance building energy performance. Innovative materials, which have become more dynamic with the development of technology, attract the attention of researchers and the building sector with their features, such as responding to environmental conditions, being recyclable, generating energy, storing energy, and utilizing climate elements such as the sun with passive or active methods. PCM and TIM, innovative building materials,

offer passive solutions by using solar energy. These innovative materials are used to create new adaptable building envelopes, allowing an active interaction with the environment to improve building energy performance.

Stritih & Novak [28] investigated a wall system consisting of a transparent insulating material and a transparent insulating material on the outside and a black paraffin PCM filled in a transparent plastic container made of polycarbonate. Manz et al. [29] proposed a two-layer passive wall system combining salt hydrate PCM and polymethylmethacrylate (PMMA) TIM. The thermal performance of the wall system, which is configured as a TIM-PCM wall filled into glass bricks from outside to inside, was investigated in the climatic conditions of Zurich, Switzerland. Many studies have investigated the performance of similar wall configurations, different transparent insulation and PCM, and material thicknesses in different climatic zones [30–33]. Unlike the translucent use of a latent heat storage wall, Heim & Klemm [34] analyzed the thermal performance under winter conditions of a transparent insulated latent heat storage solid wall consisting of a TIM and a PCM-ceramic composite. As a result of the analysis, it was found that the installed wall system significantly reduced day and night temperature fluctuations. Heim [35] examined the performance of the wall configuration in both summer and winter climatic conditions and concluded that it performed better in winter.

According to literature research, the TIM-PCM wall significantly impacts indoor temperature fluctuations, maintains comfortable temperatures, reduces heating or cooling loads, and results in energy savings. However, previous studies have generally focused on the translucent TIM-PCM wall. Studies on using TIM-PCM wall as an opaque exterior wall are very limited. PCM was commonly used in these studies by impregnating it in the wall material. Since the use of PCM by embedding into the building element is easier to apply in the field and does not require special labor, such as producing a new material before application, studies in this field were investigated. As a result of the research, the lack of sufficient resources revealed the gap in this field. This study will fill the gap in the literature by analyzing the thermal performance of the opaque TIM-PCM wall formed by the integrated use of a transparent insulating unit formed by aerogel filling between two float glass and a brick wall in which the PCM is embedded in the cavity in the clay brick. Furthermore, in some studies [36–40] where TIM was used in front of the wall, it was found that there was a danger of overheating of the wall surface, especially during the summer season. In order to prevent overheating, an air gap was used to balance the heat flow generated by sunlight between the insulation layer and the wall. In this study, the air layer is used as an additional region, and the innovative wall is named the TIM-AG-PCM wall. In order to prevent overheating by balancing the heat flow generated by sunlight between the insulation layer and the wall, an air gap was used. In this study, the air layer is used as an additional region and the innovative wall is named as TIM-AG-PCM wall.

The TIM-AG-PCM wall performance was evaluated in the Ankara province of Türkiye, where continental climate characteristics were observed. The reason for selecting Ankara province, which has a continental climate, is that PCM shows better building energy performance in regions with high day and night temperature differences [41–43]. The performance of the wall system to be analyzed is significantly affected by the operation of the PCM. For this purpose, a code was developed in MATLAB using a one-dimensional explicit finite difference method to select the material suitable for Ankara climate conditions and evaluate the effect of the wall performance on Q, DF, and TL. In the developed code, Bulut et al. [44] and Bulut et al. [45] were utilized to obtain instantaneous data at the specified time and location step. The mathematical models developed in these studies enabled adding functions to the MATLAB code from which climatic data forecasts can be obtained. Analyses were performed for both heating and cooling seasons. The study aims to develop an exterior façade system that supports the production of high energy performance and low carbon emission buildings in the continental climate zone where day and night temperature differences are high.

2. Methodology

2.1. Introduction of the TIM-AG-PCM wall

In this study, firstly, previous studies are taken as a reference to determine the location and application details of the materials to be used in the multilayer wall component, which will determine the optical and thermophysical properties of the building envelope. Regarding the ordering of the layers of TIM-AG-PCM wall systems, Kienzl [30] argued that ordering the layers according to their functions would be more efficient in terms of performance. The outer layer has the element that protects the thermal insulation

Table 1
Thermal properties of the materials of the external wall of the building.

	X (cm)	k [W/m.K]	C_P [J/kg.K]	ρ_{solid} [kg/m^3]	ρ_{liquid} [kg/m^3]
Tempered Glass	0.4	0.81	800	2225	–
Plaster	2	0.3	1050	1800	
Aerogel(Granul)	1.6	0.012	1150	120	–
Glass	0.4	1.05	840	2500	–
Air Gap	2	0.025	1007	1184	–
Brick	12	0.32	840	600	–
XPS	5	0.031	1380	24	–
RT10HC	8,5	0.2	2000	880	770
RT18HC	8,5	0.2	2000	880	770
RT21HC	8,5	0.2	2000	880	770
RT22HC	8,5	0.2	2000	760	700
RT28HC	8,5	0.2	2000	880	770

material from external factors (usually tempered glass material is used), the TIM to prevent heat loss inside, the air gap to provide a thermally insulated air cushion between the TIM and the wall, and the PCM in the inner layer as it is exposed to the internal environment. For this wall system, it is important to know how the PCM will be integrated. In the literature research on this subject, it has been observed that PCM is generally used in the wall system by impregnating the wall material [34,35,46]. Another method of using PCM in the wall system is embedded in the wall material. In the research on this method, studies in which the PCM is embedded in the brick body have attracted attention [47–50]. Brick was chosen for this study because it is one of the most widely used wall materials in the construction sector in Türkiye and does not require any specialized craft due to its internal cavity.

PCM-brick joint, using encapsulated PCM embedded in perforated brick [50–53], is provided. Lai and Chiang [47] investigated the outcome of adding PCM to conventionally insulated brick walls. They found that the thermal insulation effect is better during the daytime and provides more effective indoor heat conservation at night. With the knowledge gained from the literature, it was decided to investigate a TIM-AG-PCM wall based on a configuration of encapsulated PCM embedded wall, air gap and transparent insulation material.

For the TIM-AG-PCM wall, whose thermophysical properties are given in Table 1, the layers are determined as 0.4 cm glass, 1.6 cm granular aerogel, 0.4 cm glass, 2 cm air gap, 8.5 cm R1 capsule PCM (at different melting temperatures) between 12 cm bricks and 2 cm plaster from outside to inside (Fig. 1).

In the study, RT category materials belonging to Rubitherm brand at different melting temperatures as PCMs. PCMs in the RT category are organic materials. They store high latent heat in narrow temperature ranges. They are also chemically inert and have an unlimited lifetime. Compared to conventional RT materials, RTHC products with different melting temperatures in this study store 25–30 % more latent heat [54]. RT18HC (17–19 °C), RT21HC (20–23 °C), RT22HC (20–23 °C), and RT28HC (27–29 °C) materials with different melting temperature range were selected for the study.

Lumira series granular aerogel of Cabot brand was used as TIM. Lumira aerogel is a translucent material with 93 % light transmission per cm. It provides three times more thermal performance than insulation materials. In addition to its performance, Lumira aerogel is a material with low environmental impact due to its reusability and low impact on the environment during its production [55].

2.2. Climatic conditions data

TIM-AG-PCM wall thermal analysis was conducted based on weather data from Ankara, Türkiye. The location is between 39.57 N latitude and 32.53 D longitude and has an elevation of approximately 890 m above sea level. As per the Köppen-Geiger climate classification system [56], Ankara falls under Bsk (cold semi-arid climate). Fig. 2 displays Ankara's average monthly meteorological data from 1927 to 2023.

As per Fig. 2, it is observed that the highest temperature data is collected in July, and the lowest temperature data is collected in January.

The ASHRAE clear-sky model [58] was used to determine the hourly solar radiation. Since the ASHRAE solar radiation constant, atmospheric attenuation coefficient, and sky diffusion factor were obtained for the 21st of each month in the Bakırcı [59] study, January 21 for the heating season and July 21 for the cooling season were selected in this study.

2.3. Mathematical analysis

A transient simulation is performed with the MATLAB code developed to analyze the thermal effect of PCM during the day. Bulut

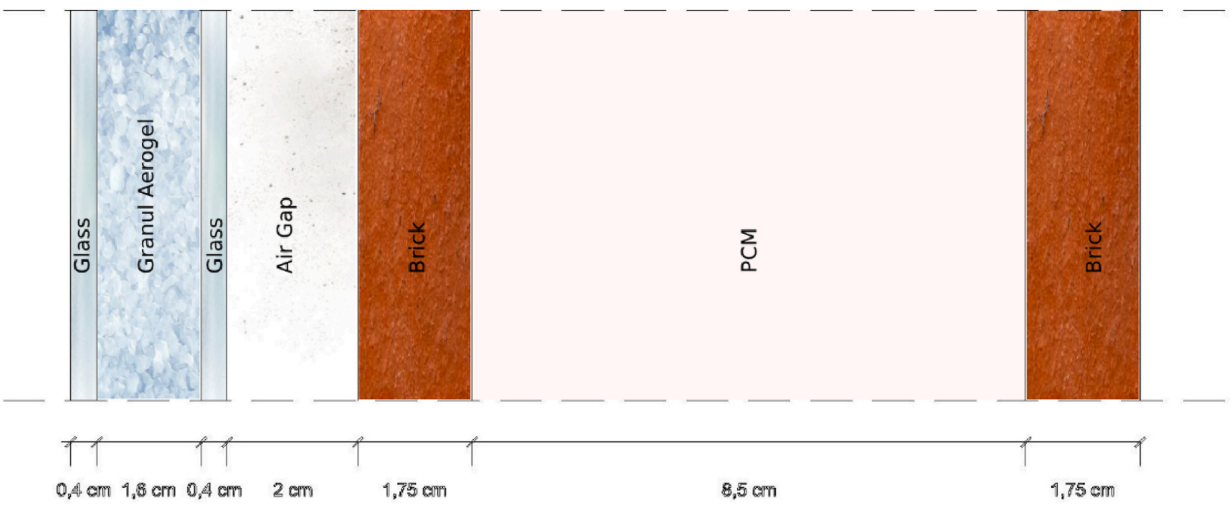


Fig. 1. TIM-AG-PCM wall cross-section.

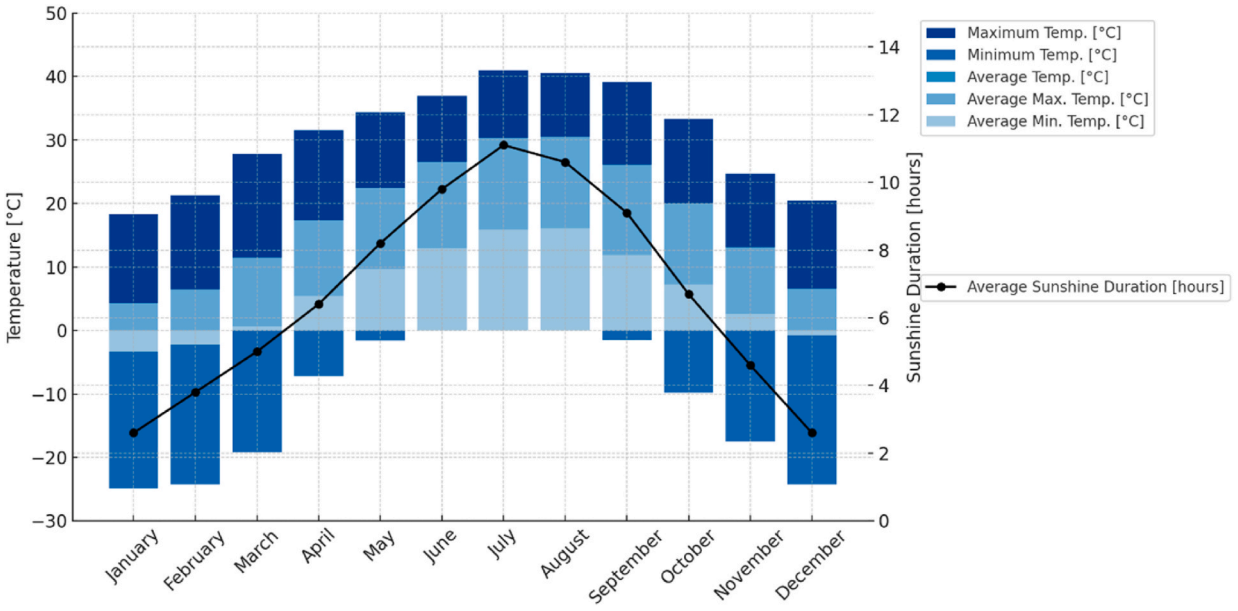


Fig. 2. Meteorological data for Ankara [57].

et al. [44] and Bulut et al. [45] were utilized for the instantaneous climate data required for transient mathematical simulation. Bulut et al. [44] created a mathematical model for daily maximum and minimum T_{db} and hourly T_{db} to simulate hourly data measured for 15 years for 78 provinces of Türkiye. Bulut et al. [45] developed a model to estimate the annual variation of global solar radiation for any location in Türkiye. The mathematical models developed in these studies enabled adding functions to the MATLAB code from which climatic data forecasts can be obtained.

To examine the thermal performance of the TIM-AG-PCM wall and compare it to the standard external wall, two different scenarios

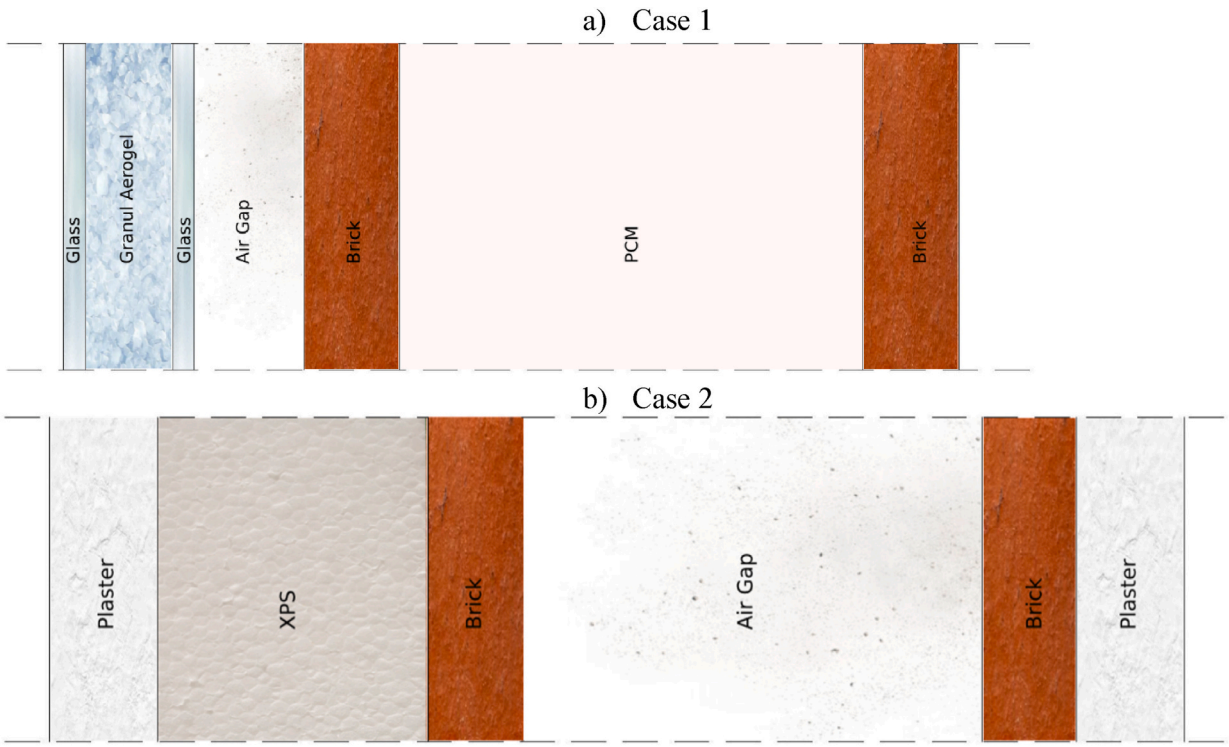


Fig. 3. a) TIM-AG-PCM wall cross-section, b) Standard wall cross-section with opaque insulation.

are examined, as depicted in Fig. 3.

One-dimensional heat transfer through the wall was presumed. Equation (1) illustrates the conduction heat transfer between building materials and PCM in the solid or liquid phase.

$$\frac{\partial T}{\partial t} = \alpha \frac{\partial^2 T}{\partial x^2} \tag{1}$$

The heat transfer during phase change, i.e., during melting/solidification, can be found in Eq. (2).

$$\frac{\partial T}{\partial t} = \alpha \frac{\partial^2 T}{\partial x^2} - \frac{L_H}{C_p} \frac{\partial f}{\partial t} \tag{2}$$

f is the proportion of liquid in the material at the time of phase change and depends on the conditions in Eq. (3) [49].

$$f(t) = \begin{cases} 0 \quad \text{if} \quad T_{pcm} \geq T_m - \dfrac{\Delta T}{2} \\ \dfrac{1}{\Delta T}\left(T_m + \dfrac{\Delta T}{2} - T_{pcm}\right) \quad \text{if} \quad T_m - \dfrac{\Delta T}{2} \leq T_{pcm} \leq T_m + \dfrac{\Delta T}{2} \\ 1 \quad \text{if} \quad T_{pcm} \leq T_m - \dfrac{\Delta T}{2} \end{cases} \tag{3}$$

In the study, the boundary conditions on the external and internal surfaces of the wall are given in Eq. (4) and Eq. (5).

$$-k \left.\frac{\partial T}{\partial x}\right|_0 = h_0 \left[T_d(t) - T_{e,wall}(t)\right] + \alpha_G I(t) + \varepsilon\sigma\left[T_{sky}(t)^4 - T_{e,wall}(t)^4\right] \tag{4}$$

$$-k \left.\frac{\partial T}{\partial x}\right|_i = h_i \left[T_{i,wall}(t) - T_{room}\right] \tag{5}$$

To ensure thermal comfort for the heating and cooling season and to reduce heat loss during the heating season, the space operative temperature is taken as 21 °C. The symbols h_o and h_i denote the heat convection coefficient between the external environment and the internal environment and the wall surface, respectively, and these values are assumed to be 22 W/m^{2}K and 9 W/m^{2}K, respectively [60].

$\alpha G = 0.6$, $\varepsilon = 0.4$ values were taken in the study [61].

The different temperature profiles obtained in the cross-section of the exterior wall of buildings at any moment of the daily period depend on the $T_{i,wall}$, T_d, and the thermophysical properties of the wall. During the propagation of this heat wave along the wall, its amplitude will decrease depending on the thermophysical properties of the wall materials. When this wave reaches the inner surface, it will have an amplitude significantly smaller than its value at the outer surface. The time it takes for the heat wave to move from the outer surface to the inner surface is called 'TL', and the rate of decrease in its amplitude during this process is called 'DF' [62–65]. The heat storage capabilities of any material are greatly influenced by the properties of TL and DF. The volume surrounded by the building element with a low reduction factor shows less oscillating temperature fluctuations in the indoor environment. Thus, a comfortable and stable indoor environment is obtained [66].

Methods such as analytical [67,68], numerical [69,70,71,72], and experimental [73,74] are often used to measure TL and DF. The DF (f) is defined as the ratio of the temperature change on the $T_{i,wall}$ to the temperature change on the $T_{e,wall}$ and is calculated from Eq. (6) [75].

$$f = \frac{{T_{i,wall}}^{max} - {T_{i,wall}}^{min}}{{T_{e,wall}}^{max} - {T_{e,wall}}^{min}} \tag{6}$$

The TL (Φ) is defined as the lag between the time when the maximum temperature occurs on the external surface of the wall and the time when the maximum temperature occurs on the internal surface (Eq. (7)) [75].

$$\Phi \begin{cases} t_{{T_{i,wall}}^{max}} - t_{{T_{e,wall}}^{max}} \ \ if \ \ t_{{T_{i,wall}}^{max}} > t_{{T_{e,wall}}^{max}} \\ 24 \ \ if \ \ t_{{T_{i,wall}}^{max}} = t_{{T_{e,wall}}^{max}} \\ t_{{T_{i,wall}}^{max}} - t_{{T_{e,wall}}^{max}} + 24 \ \ if \ \ t_{{T_{i,wall}}^{max}} < t_{{T_{e,wall}}^{max}} \end{cases} \tag{7}$$

The wall material's thermophysical properties can make it possible to store solar energy and transfer it to the interior space with a certain time delay. In this case, the TL and DF are determining the building's thermal energy storage. In regions with large daily temperature variations, determining TL and DF is essential for reducing the heating and cooling load in energy-efficient building design [76].

2.4. Simulation

A two-dimensional simulation of the TIM-AG-PCM wall cross-section was performed by HTflux software using the same boundary conditions and material properties as the mathematical analysis. The instantaneous outdoor temperature data obtained with MATLAB were transferred to HTflux, and transient thermal simulation was performed.

The HTflux tool used for thermal simulation is a software certified by EN ISO 10077–2:2007 and EN ISO 10211–2:2012. Bienvenido-Huertas et al. [77] calculated 2D simulation of five patented slab-to-facade thermal bridges, Purwanto [78] analyzed the heat transfer of roof constructions with different cladding materials, Alkadri et al. [79] analyzed the dynamic thermal bridges of the south-facing wall of a café inside a library building in Indonesia with the HTflux simulation tool. In addition to the validation of the HTflux simulation tool by standards, it has been used as a simulation tool in many scientific studies where mathematical analysis and experimental studies have been performed, which has been effective in the validation and reliability of this software tool.

The choice of HTflux in the study is based on its user-friendly interface and its ability to efficiently handle transient heat transfer simulations, which are critical for accurately capturing the phase change behavior of PCM materials. While tools such as EnergyPlus are widely used for whole-building energy simulations, they are less suited for detailed analysis of localized heat transfer phenomena. On the other hand, advanced numerical simulation tools like ANSYS Fluent or COMSOL Multiphysics, although highly precise, require significantly higher computational resources and expertise, making them less practical for this study's scope. HTflux offers a balanced approach, providing both computational efficiency and the capability to model phase change processes effectively. Therefore, it was deemed an appropriate and efficient choice for the objectives of this research.

The 2D transient thermal simulation of the TIM-AG-PCM wall was performed for the heating and cooling season of January 21 and 21 July. The same boundary conditions and material properties were used as in the analysis performed with MATLAB. The simulation was carried out in three periods with a time step of 10 min. On a broad color scale, the thermal analysis displays the temperature distribution of the wall layers. The temperature is characterized by a range of −5 °C–35 °C, with the red color indicating the highest and the blue color indicating the lowest.

Instantaneous temperature distribution and heat flux data were obtained by transient thermal simulation in HTflux, and the TL, DF, and total amount of heat transferred (Q) of the TIM-AG-PCM wall was calculated. As a result, the TIM-AG-PCM wall was evaluated by comparing the TL, DF, and E data obtained in MATLAB code.

2.5. MRT analysis

Thermal performance in energy-efficient building design is based on meeting indoor thermal comfort with minimum energy consumption. The MRT is one of the factors that impact thermal comfort indoors [58,80]. MRT is the temperature used to measure the radiant heat exchange between the user and the surrounding surfaces. It depends on the position of the user in terms of volume, posture, and temperature of the neighboring surfaces. These parameters affecting MRT can cause the surface temperatures adjacent to the volume to vary significantly, complicating the analysis [81].

The effect of the temperature data obtained as a result of mathematical analysis on indoor thermal comfort was evaluated with the average radiant calculation. For this assessment, a tool developed by researchers at the Center for the Build Environment (CBE) at the University of Berkeley was used to calculate and display the MRT and the estimated comfort in a space based on room surface temperatures sunlight gain through windows and skylights. An imaginary room (Fig. 4) with dimensions of 3m × 5m x 3m (widthxlengthxheight) was added to the online tool. The $T_{i,wall}$ data of the transparent insulated hidden heat storage wall on the south wall of the room and the standard wall on the other facades were entered. A seated person was assumed to be located 0.7m × 1m in the southeast direction and 4m × 1m in the northeast direction of the room.

Mathematical analysis data were used for the instantaneous $T_{i,wall}$ of the TIM-AG-PCM wall and the standard wall during the heating and cooling season. MRT calculation of the position steps was determined by inputting hourly Ti, and wall data was performed

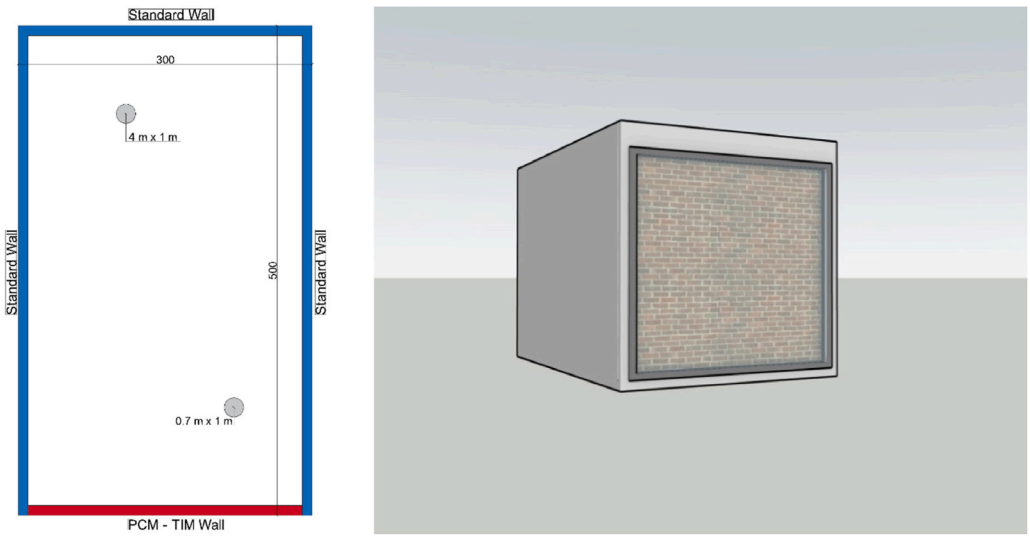


Fig. 4. Imaginary room for the MRT Analysis.

on the walls.

3. Results and discussion

3.1. Validation

The code developed in MATLAB was verified with the results obtained by Arıcı et al. [82] for Case 3, where the latent heat of seven different scenarios with PCMs at different locations and different melting temperatures in the wall cross-section were analyzed mathematically. A PCM with a melting temperature of 25 °C, a melting temperature of 2000 (J/kg.K), and a thickness of 30 mm was used. The results were compared using the daily variation of T_{out} and solar radiation of Kocaeli province. The indoor temperature was 24 °C, and the indoor convection h was 7.7 (W/m^2K). The comparison of the results obtained with the code developed in this study and the results in the study of Arıcı et al. [82], is given in Fig. 5. According to the figure, the results obtained agree with the reference study, with an average deviation of 0.8 %.

The Courant-Friedrichs-Lewy (CFL) condition [83] was employed to ensure the stability and convergence of the numerical model by maintaining an appropriate relationship between spatial and temporal resolutions. The maximum thermal diffusivity, $t_{diff,max}$, was determined as 6.3492×10^{-7} m^2/s. While determining the spatial step, the layer thicknesses of the wall were considered. A spatial step divisible by the layer thicknesses was selected to ensure accurate temperature data collection from each layer. Prior to this selection, a graph of the inner surface temperature of the final layer was generated for different Δx values (0.001, 0.002, 0.004) (Fig. 6).

The analysis conducted for different Δx values revealed no significant variations in the temperature values at the same spatial locations (Fig. 6). Therefore, for further analyses, a spatial step of 0.004 was selected, and a time step of 1.2 s, determined using the CFL condition (CFL $\leq \Delta x$), was adopted for this spatial resolution.

3.2. Selection of the PCM

The high thermal performance of the TIM-AG-PCM wall during the heating and cooling season depends on the selection of the suitable PCM. For this reason, firstly, using the meteorological data of Ankara province dated 21 January and 21 July, the state change states of PCMs on these dates were examined with the code developed in MATLAB.

The behavior of PCMs with different melting temperatures at the heating climate condition on 21 January is shown in Fig. 7. The T_{PCM} curve given in the graph gives the hourly temperature reached by the cavity in the clay brick body.

In these graphs, the line shown in blue represents the temperature change of the cell containing the PCM for one day. In the area between the melting temperature lines of materials with different melting temperatures and the points where the temperature lines of the cell coincide, the material shows phase change. In the graphs prepared for the heating season, RT18HC material changes from liquid phase to solid phase during the night hours when the T_{out} is the lowest, and the T_{room} also decreases and changes from solid phase to liquid phase around 14.00 when the outdoor temperature and room temperature increase. Therefore, RT18HC material was selected for the heating season performance analysis.

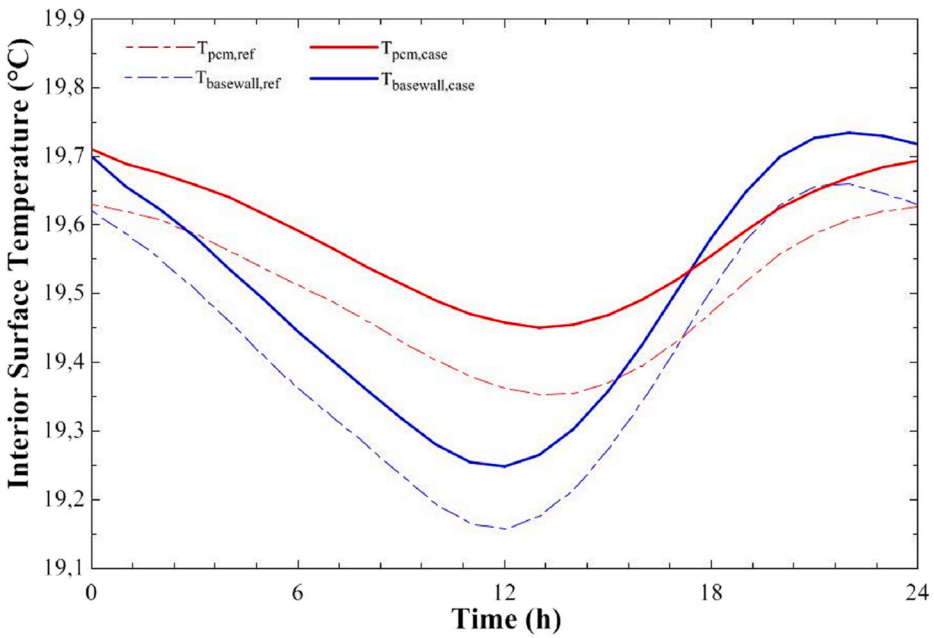


Fig. 5. The validation of the MATLAB code model.

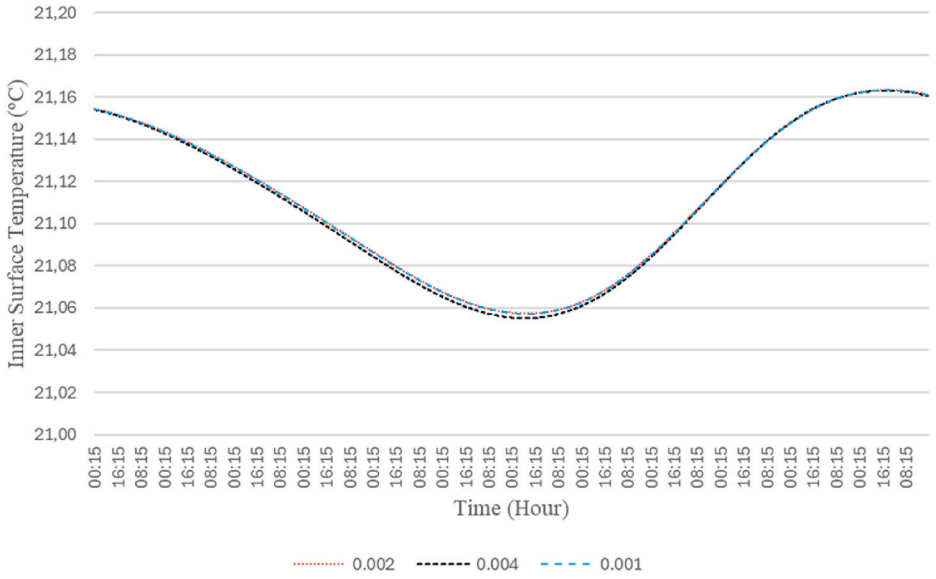


Fig. 6. Comparison of Δx values.

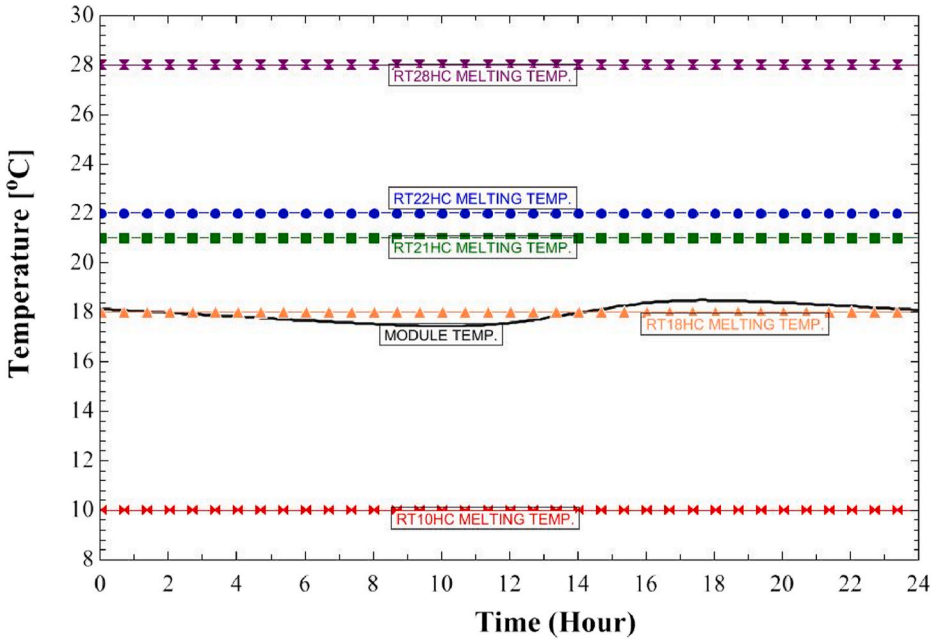


Fig. 7. (a) RT10HC, (b) RT18HC, (c) RT21HC, (d) RT22HC, (e) RT28HC phase change state of PCMs during the heating season.

Fig. 8 depicts the PCMs' behavior during the cooling season on July 21st.

In the graph (Fig. 8), the blue line represents the temperature fluctuations of the cell containing the PCM during the day as in the heating season. The working state of the material that changes phase in the face of these temperature fluctuations is given by the area between the points where the line showing the melting point and the line showing the cell temperature coincide. According to Fig. 8, it is seen that the RT22HC material with a melting temperature of 22 °C changes state from liquid phase to solid phase near sunrise (around 6 o'clock) when the outdoor temperature and room temperature decrease and from solid phase to liquid phase around 12.00 when the T_{out} and T_{room} increase. For this reason, RT22HC material was selected for the performance analysis to be performed for the cooling season on 21 July.

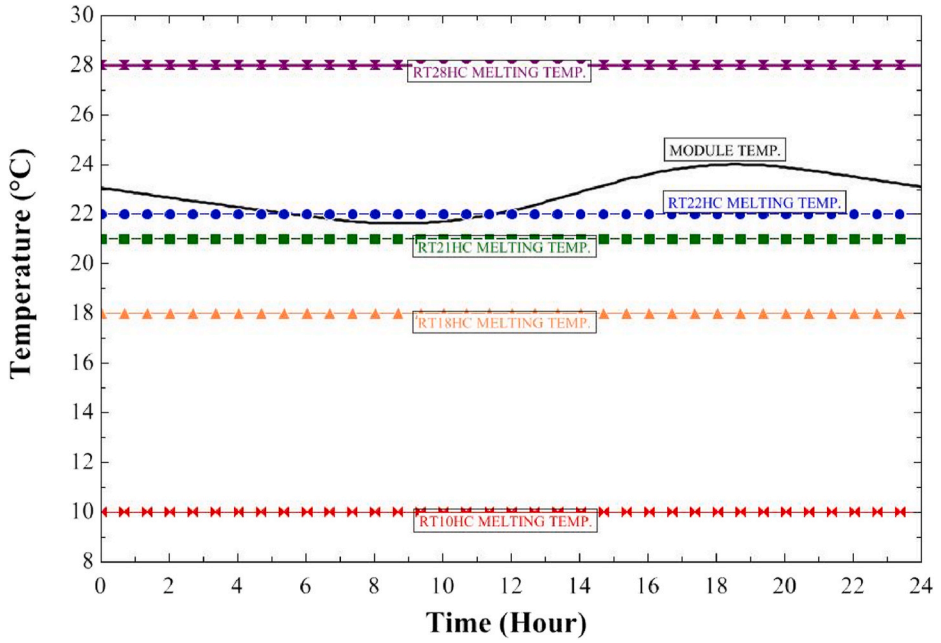


Fig. 8. (a) RT10HC, (b) RT18HC, (c) RT21HC, (d) RT22HC, (e) RT28HC phase change state of PCMs during the cooling season.

3.3. Thermal performance of TIM-AG-PCM wall: heating season

It is known that the combined use of PCM and TIM reduces temperature fluctuations during the day, thus reducing energy consumption by keeping the T_{room} close to the comfort temperature. $T_{i,wall}$ graphs of the TIM-AG-PCM wall and the standard external wall obtained as a result of the mathematical analysis are given in Fig. 9 for the heating condition, respectively.

It was determined that the maximum $T_{i,wall}$ of the RT18HC integrated TIM-AG-PCM wall increased by 4.5 °C and the $T_{i,wall}$ amplitude decreased by 1.7 °C compared to the maximum $T_{i,wall}$ of the standard wall for the heating conditions. The amplitude of the $T_{i,wall}$ indicates the difference between the maximum and minimum values of the wall's $T_{i,wall}$. The TIM-AG-PCM wall has a lower $T_{i,wall}$ amplitude than the standard wall, which suggests that indoor temperature fluctuations are also reduced.

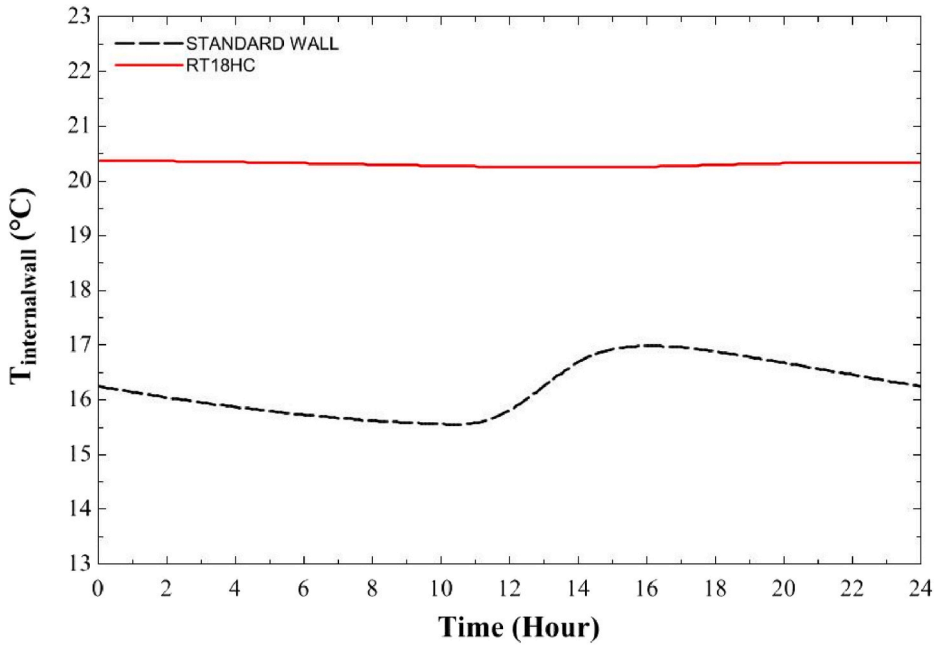


Fig. 9. $T_{i,wall}$ in the heating season.

In addition to heat transfer, the DF and TL parameters were also investigated. The RT18HC integrated TIM-AG-PCM wall's external and internal surface temperatures fluctuate in heating conditions during a 24-h season (Fig. 10).

The $T_{i,wall}$ amplitude of the RT18HC integrated TIM-AG-PCM wall was determined to be about 0.13 °C and the external surface temperature amplitude was determined to be 6.05 °C. The DF, defined as the ratio of the amplitude of the $T_{i,wall}$ change to the amplitude of the $T_{e,wall}$ change, was determined as 0.02. The phase difference TL, defined as the time difference between the time when the maximum temperature occurs on the external surface of the wall and the time when the maximum temperature occurs on the internal surface, was found to be 10.27 h.

For the standard wall, the external and internal T_{surf} change over 24 h is given in Fig. 11.

For the heating season in Ankara, the DF was determined to be 0.26 and the TL to be 1.54 h for the standard external wall. Accordingly, it was determined that the DF decreased by 0.24 by using the RTI8HC integrated TIM-AG-PCM WALL instead of the standard wall for Ankara heating conditions. It is also seen that there is an additional TL of 8.33 h with the use of the RT18HC integrated TIM-AG-PCM WALL.

By mathematical analysis, the thermal performance of the TIM-AG-PCM wall was assessed and compared to the standard wall. The instantaneous temperature data of the TIM-AG-PCM wall taken in MATLAB were transferred into the HTflux simulation tool, and its dynamic thermal performance was simulated without changing the boundary conditions and material properties. As a result of the simulation, hourly temperature data and visualizations showing the temperature flow in the wall section were obtained. The images taken for each 10-min time interval and the images at low and high-temperature periods are shown in Fig. 12.

The hourly temperature data obtained from the transient thermal simulation were exported and graphed (Fig. 13). In the simulation for the heating season of the TIM-AG-PCM wall, it is seen that the $T_{i,wall}$ of the wall does not fall below the comfort temperature during the day. During the night hours when the T_{air} dropped, the $T_{i,wall}$ was measured to be close to 20 °C. The fact that the $T_{i,wall}$ curve did not fluctuate revealed that the TIM-AG-PCM wall was successful in thermal efficiency heating conditions.

TL and DF calculations were made from the instantaneous temperature data obtained from the simulation. The $T_{i,wall}$ amplitude of the RT18HC integrated TIM-AG-PCM wall is about 0.15 °C, and the $T_{e,wall}$ amplitude is 5.9 °C. The DF, defined as the ratio of the amplitude of the $T_{i,wall}$ change to the amplitude of the $T_{e,wall}$ change, is 0.026. The phase difference TL, defined as the time difference between the time when the maximum temperature occurs on the external surface of the wall and the time when the maximum temperature occurs on the internal surface, is 11 h.

The comparison of the mathematical analysis performed in MATLAB program and the transient thermal simulation performed in HTflux software to evaluate the thermal efficiency of the TIM-AG-PCM wall over TL and DF at 21 January heating condition is given in Table 2.

When the data obtained from the mathematical analysis and simulation for DF and TL are compared, it is seen that there is a significant consistency of 70 % in the DF results and a 33-min time shift difference in the TL results. When the amount of heat transferred from the wall is compared, it is 6.21 W/m^2 on average according to the mathematical analysis result and 5.89 W/m^2 on average according to the transient thermal simulation result. The analysis results are consistent, with a significant rate of approximately 95 %. This agreement reveals the success of the TIM-AG-PCM wall in terms of thermal performance during the heating season.

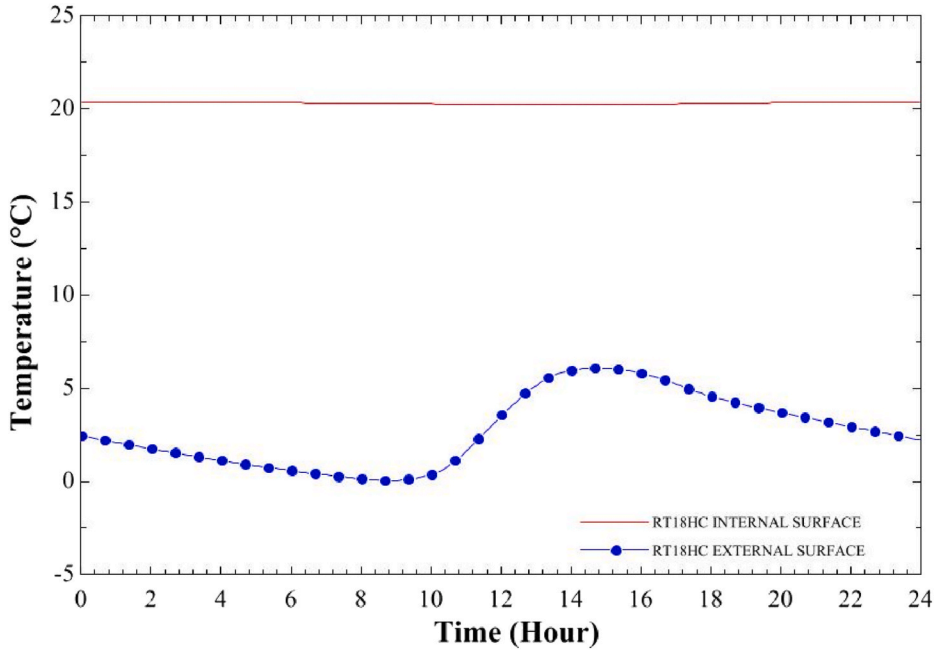


Fig. 10. The internal and external T_{surf} of the standard wall for Ankara in heating season.

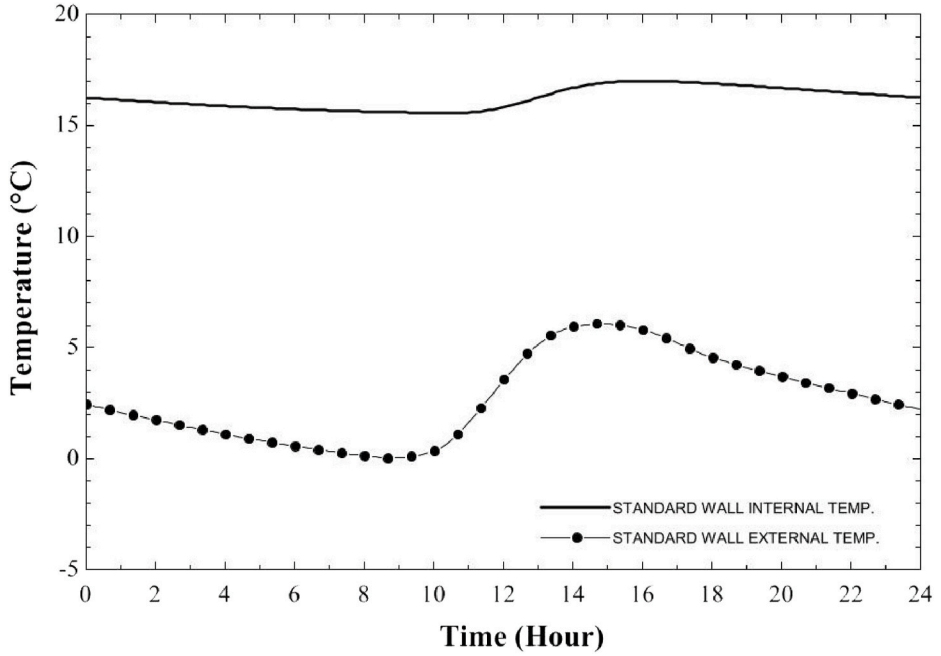


Fig. 11. The internal and external T_{surf} condition of the standard wall for Ankara in heating season.

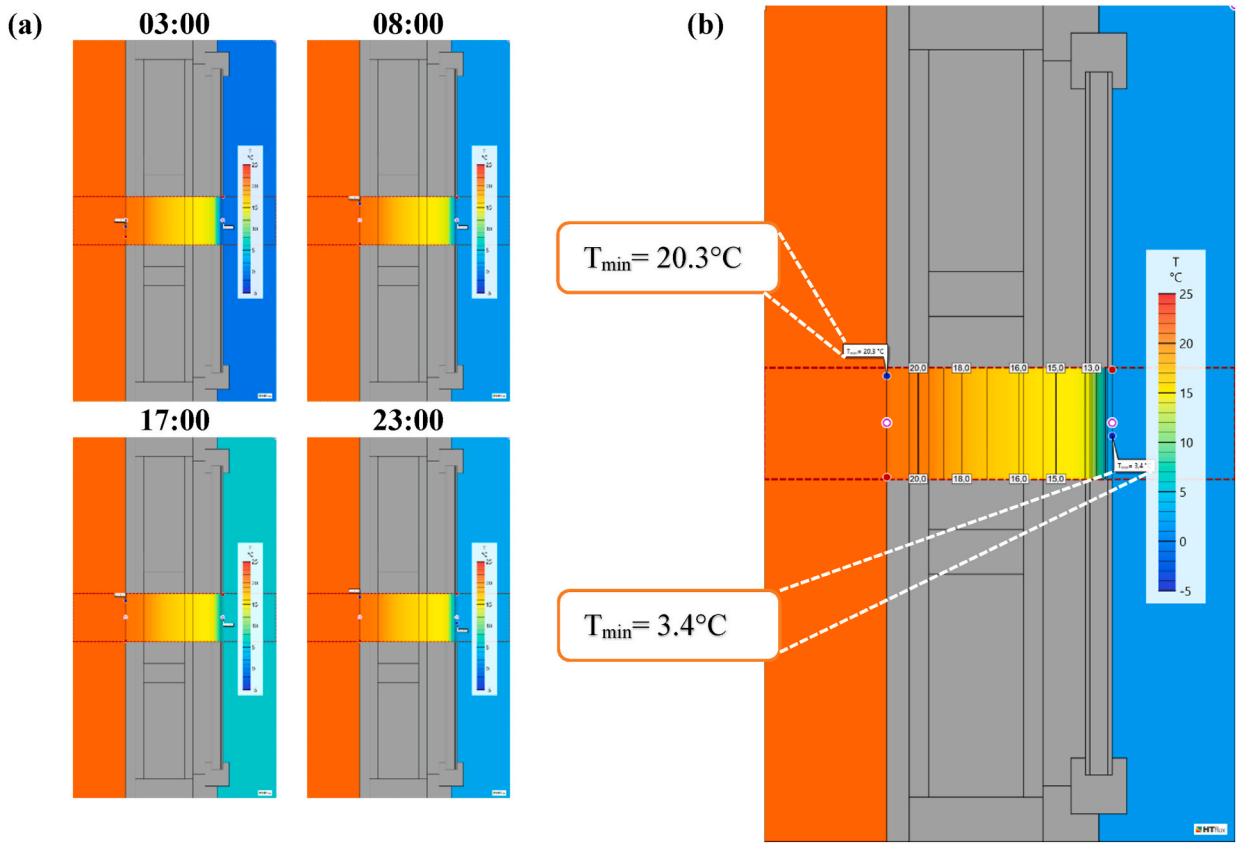


Fig. 12. (a) Temperature variation of the TIM-AG-PCM wall on 21 January (b) Extended part of the dynamic thermal simulation result of the TIM-AG-PCM wall (08:00).

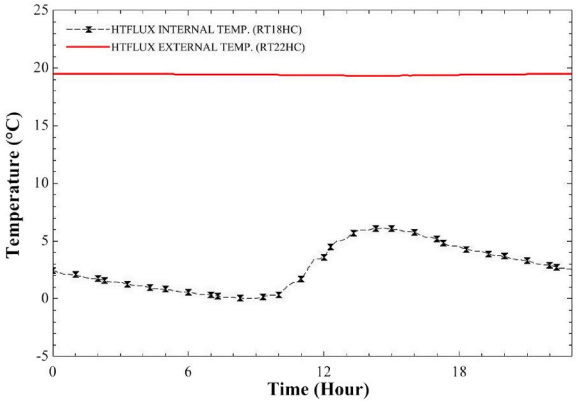


Fig. 13. Internal and external T_{surf} of the TIM-AG-PCM wall for the heating season HTflux data.

Table 2
DF and TL data of TIM-AG-PCM wall heating condition.

TIM-AG-PCM wall	DF (°C)	TL (Hour)
Matlab Analysis Data	0,02	10.27
HTflux Simulation Data	0,026	11

3.4. Thermal performance of TIM-AG-PCM wall: cooling season

The $T_{i,wall}$ graphs of the TIM-AG-PCM wall and the standard external wall obtained as a result of the mathematical analysis are given in Fig. 14.

It can be observed that in the cooling season, the maximum $T_{i,wall}$ of the RT22HC integrated TIM-AG-PCM wall is 1.15 °C, and the $T_{i,wall}$ amplitude is 3.36 °C less than the maximum $T_{i,wall}$ of the standard wall. The fact that the $T_{i,wall}$ peak value of the TIM-AG-PCM wall is lower than the standard wall indicates that it will reduce energy consumption during the cooling season.

Fig. 15 displays the changes in external and internal T_{surf} of the TIM-AG-PCM wall with integrated RT22HC material during the cooling season in Ankara province.

The DF of the RT22HC integrated TIM-AG-PCM wall was calculated to be 0.021, with an $T_{i,wall}$ amplitude of approximately 0.26 °C and an $T_{e,wall}$ amplitude of 12.03 °C. The TL, defined as the time difference between the time when the maximum temperature occurs on the external surface of the wall and when the maximum temperature occurs on the internal surface, was found to be 7.08 h.

As shown in Fig. 16, the cooling condition of the standard wall involves a change in the external and internal surface temperature over 24 h.

The DF was found to be 0.26, and the TL was found to be 2.3 h for the standard exterior wall during the cooling season in Ankara. According to this, the DF decreased by 0.24, and there was a TL of 4.38 h when using the RT22HC integrated TIM-AG-PCM wall instead of the standard wall for Ankara under heating season.

The instantaneous temperature data of the TIM-AG-PCM wall for the 21 July cooling season obtained from MATLAB were transferred into the HTflux simulation tool, and its transient thermal performance was simulated without changing the boundary conditions and material properties. For each moment of the 10-min time step, the images of the moments when the weather is hot during the day and when the air temperature drops at night are taken from Fig. 17.

In the instantaneous data (Fig. 18) of the simulation performed for the cooling season of the TIM-AG-PCM wall, it was noted that the $T_{i,wall}$ of the wall did not temperature fluctuate during daytime hours when the air temperature reached 30 °C and at night when the T_{air} decreased, and it was almost constant at the comfort temperature.

TL and DF calculations were performed to measure the thermal efficiency of the TIM-AG-PCM wall under cooling conditions. The $T_{i,wall}$ amplitude of the RT22HC integrated TIM-AG-PCM wall was determined to be about 0.3 °C, and the external surface temperature amplitude was determined to be 11.7 °C. The DF of the TIM-AG-PCM wall was determined as 0.027. The TL of the wall was found to be 8.4 h.

The comparison of the mathematical analysis performed in the MATLAB program and the transient thermal simulation performed in the HTflux software for the evaluation of the thermal efficiency of the TIM-AG-PCM wall over TL and DF in the 21 July cooling season is given in Table 3.

The data obtained by different analysis methods using the same boundary conditions and the same material properties of the TIM-AG-PCM wall are compared and analyzed in Table 3. It is observed that there is about 70 % agreement in DF results and a 28-min TL difference shift in TL results. When the amount of heat transferred through the wall is compared, it is 2.39 W/m^2 on average according to the mathematical analysis result and 2.29 W/m^2 on average according to the transient thermal simulation result. The conclusions of the two analyses agree by a significant margin of about 95 %. The ratios obtained in the comparative analysis reveal that the TIM-AG-

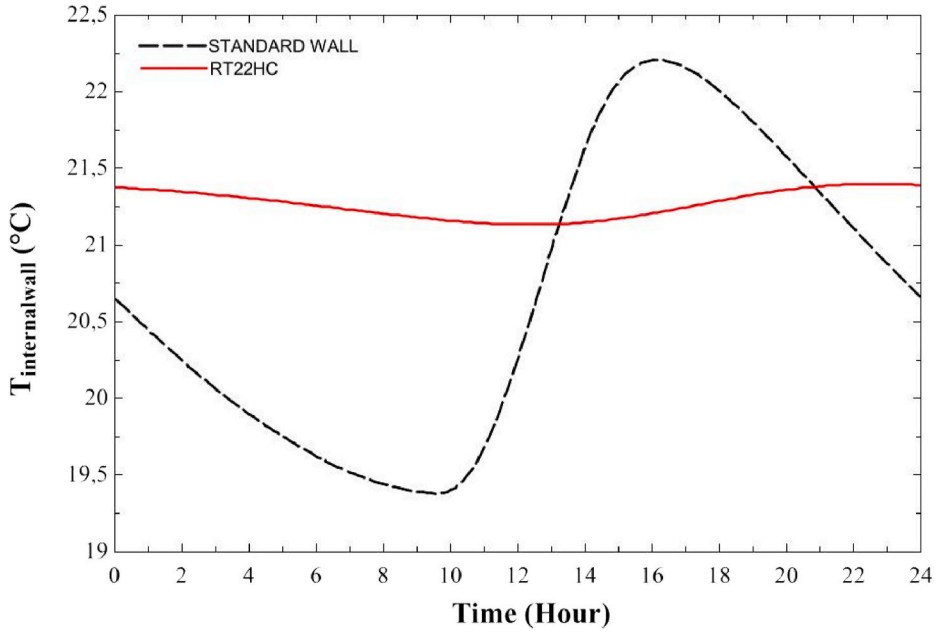


Fig. 14. $T_{i,wall}$ in the cooling season.

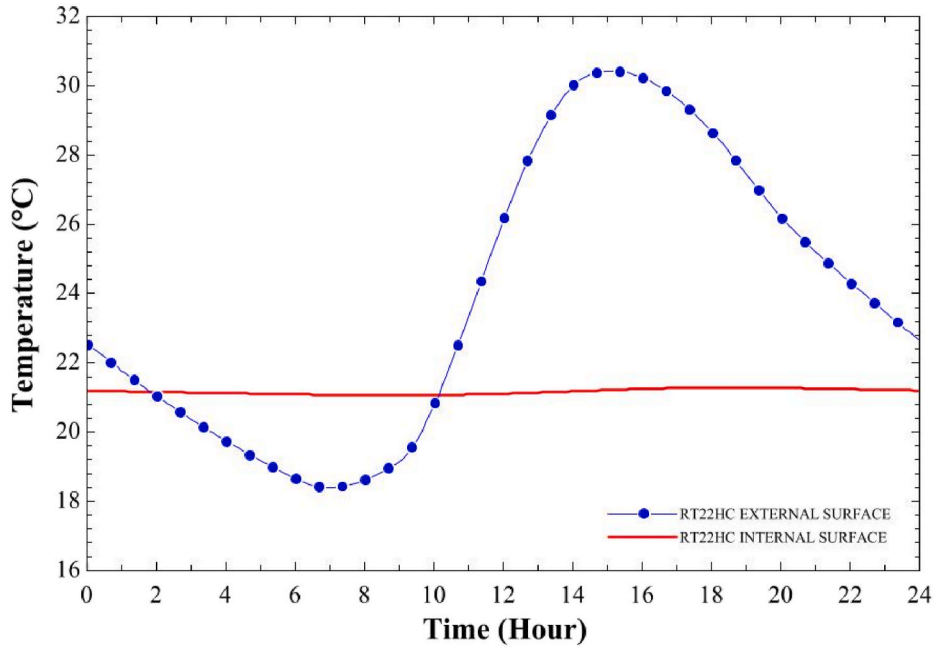


Fig. 15. Condition of internal and external T_{surf} of RT22HC material for Ankara in the cooling season.

PCM wall will positively affect the building energy performance in the cooling season.

A comparative analysis was conducted to evaluate the thermal performance of the TIM-AG-PCM wall system under Ankara's climatic conditions relative to the findings of Bilgin and Arıcı [71]. In their study, Bilgin and Arıcı analyzed a PCM-integrated opaque insulated wall system and reported thermal load reduction (TL) values of 16.11 and 8.43 for the cooling and heating seasons, respectively. Their corresponding decrement factor (DF) values were 0.032 and 0.072. In contrast, the TIM-AG-PCM wall system presented significantly improved thermal performance. For the cooling season, the TIM-AG-PCM system demonstrated a TL value of 7.08 and a DF value of 0.021, indicating a notable reduction in thermal load and improved energy efficiency. Similarly, during the heating season, the TIM-AG-PCM wall achieved a TL value of 0.02 and a DF value of 10.27. These results reveal the superior

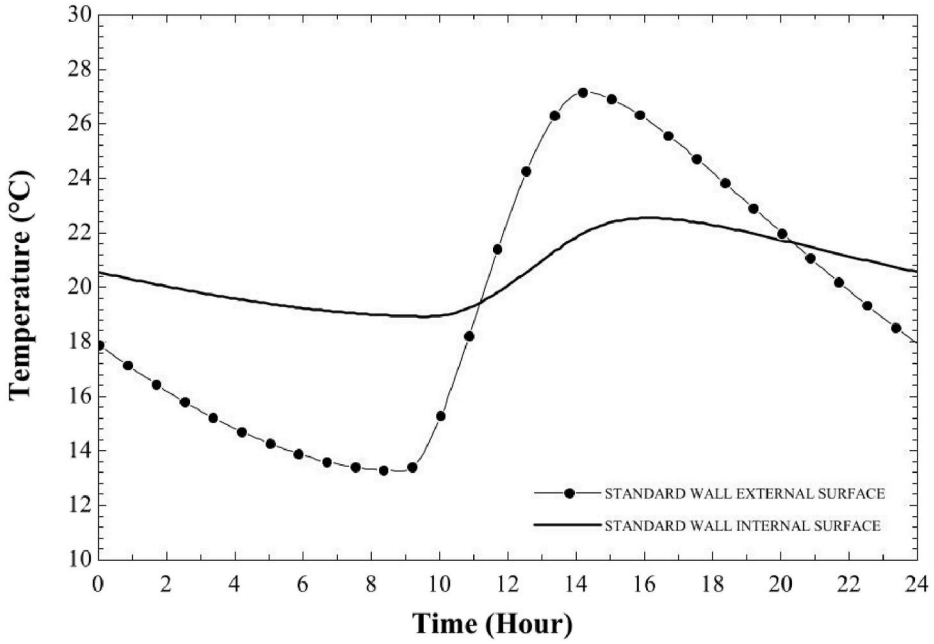


Fig. 16. Condition of the standard exterior wall for Ankara in cooling season: internal and external T_{surf}.

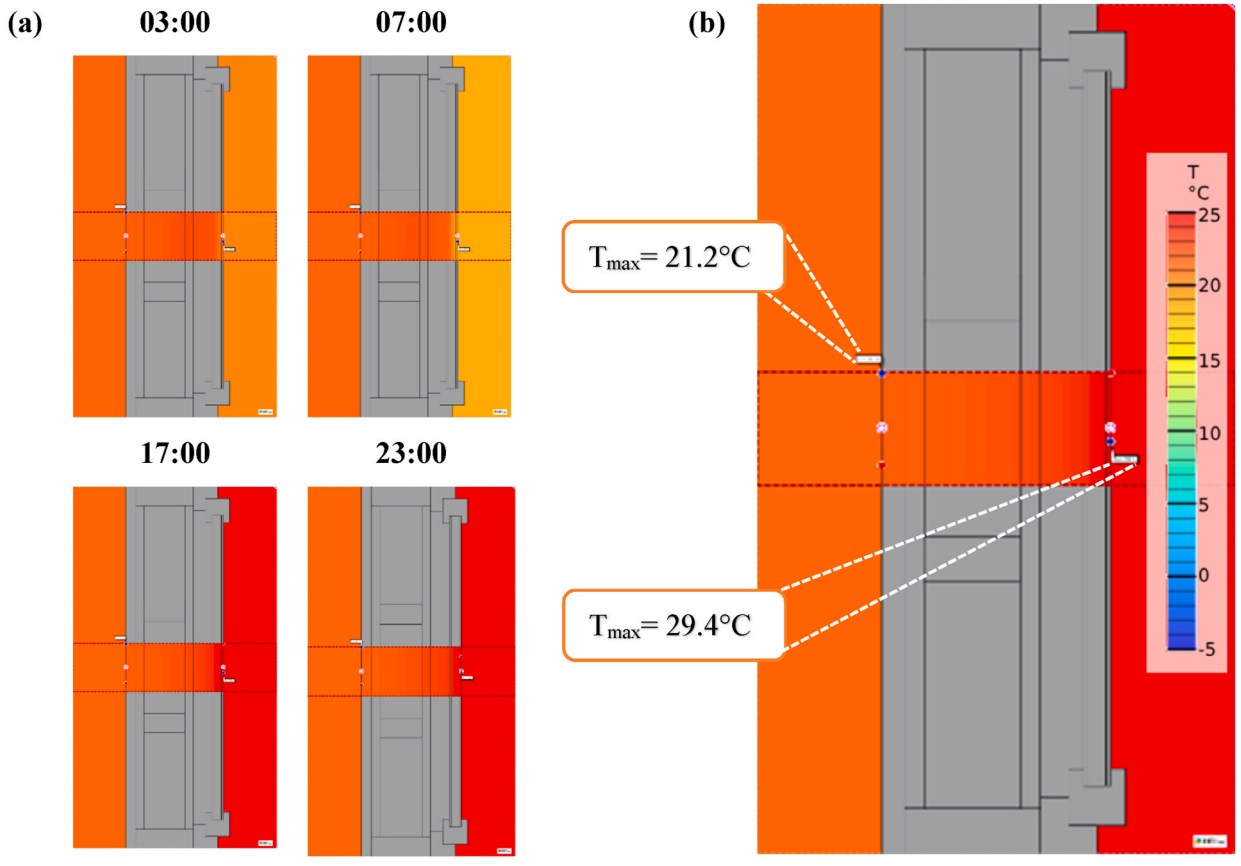


Fig. 17. (a) Temperature variation of the TIM-AG-PCM wall on 21 July (b) Extended part of the transient thermal simulation result of the TIM-AG-PCM wall (17:00).

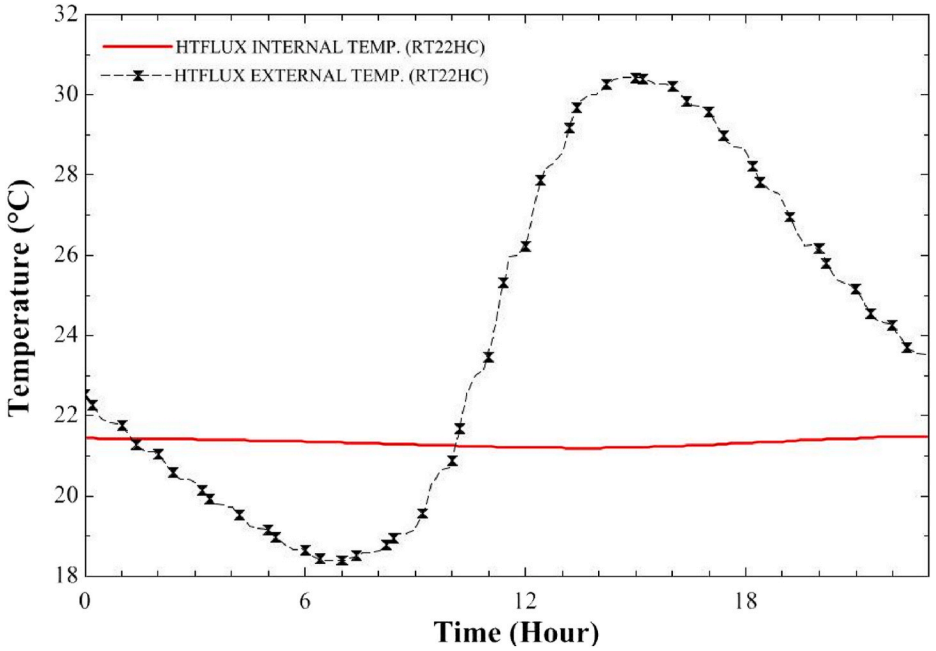


Fig. 18. Internal and external T_{surf} of the TIM-AG-PCM wall for the cooling season HTflux data.

Table 3
DF and TL data of TIM-AG-PCM wall cooling season.

TIM-AG-PCM wall	DF (°C)	TL (Hour)
Matlab Analysis Data	0,021	7,08
HTflux Simulation Data	0,027	8,4

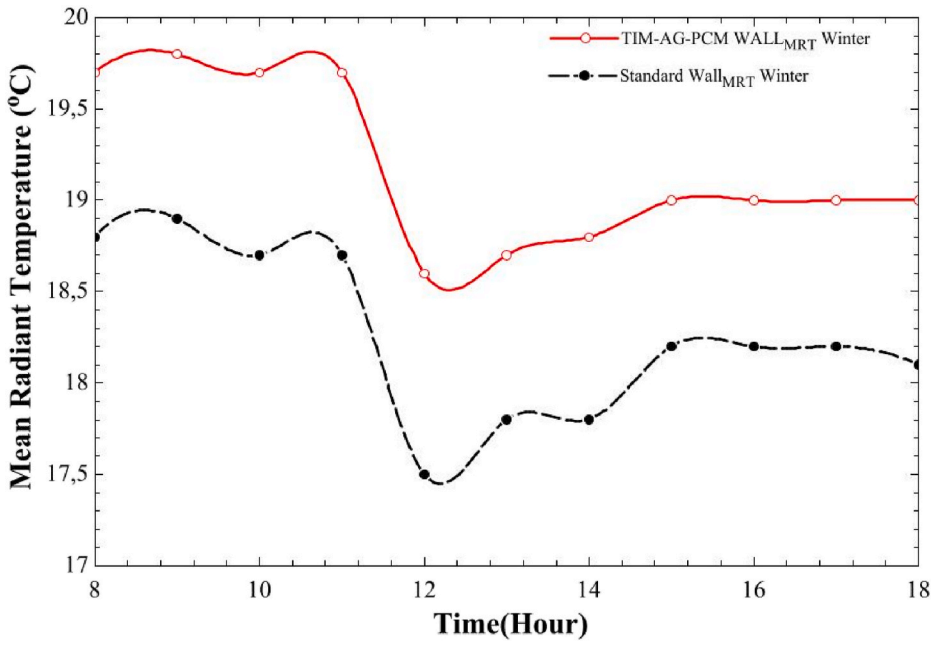


Fig. 19. MRT values of a room consisting of TIM-AG-PCM wall and standard wall installation for Ankara heating season.

performance of the TIM-AG-PCM wall system, particularly in reducing thermal load and moderating indoor temperature fluctuations during both cooling and heating seasons. The integration of transparent insulation material (TIM) alongside PCM contributes to this enhanced thermal performance by providing additional insulation and leveraging the phase-change properties of the PCM layer. This comparison underscores the potential of the TIM-AG-PCM wall as a more effective alternative to conventional PCM-insulated wall systems, especially in regions with climatic conditions similar to Ankara.

3.5. Effect of TIM-AG-PCM wall on thermal comfort

The effect of the transparent insulated latent heat storage wall on indoor thermal comfort is also analyzed through the MRT parameter. Assuming that there is a transparent insulated latent heat storage wall on the south wall, the $T_{i,wall}$ value of this wall was entered into the simulation tool where the analysis was performed, and the $T_{i,wall}$ measurements of the standard wall were entered for the walls on the other facades. I_t values obtained from the MATLAB code are entered. Azimuth and Altitude values calculated mathematically according to latitude and time of day were entered.

The analysis for heating conditions (Fig. 19) shows that the graph curve at the 0.7 m × 1 m position step where the transparent insulated latent heat storage wall and the standard wall intersect is close to the indoor thermal comfort temperature of 21 °C. It also reveals that the fluctuation is less than the graph curve at the 4 m × 1 m location step where the standard wall and the standard wall intersect. The increase in MRT value before and after 12.00 at the 0.7 m × 1 m location step where the transparent insulated wall is located is thought to be due to the change of state of the PCM. This reveals that the transparent insulated latent heat storage wall has a positive effect on indoor thermal comfort during the heating season.

The analysis for the cooling season (Fig. 20) shows that the intraday temperature fluctuations of the 4 m × 1 m location step graph curve at the intersection of the standard wall, and the standard wall ia steeper than the 0.7 m × 1 m location step graph curve at the intersection of the transparent insulated latent heat storage wall and the standard wall. Between 12:00 and 14:00, when the outdoor temperature is the highest, the TIM-AG-PCM wall system shows a curvilinear performance close to the indoor comfort temperature. It shows a positive effect on the cooling season.

4. Conclusion

In this study, mathematical analysis and transient thermal simulation of Ankara province, which has a continental climate, were carried out by considering the dates of 21 January with the lowest temperature averages for the heating season and 21 July with the highest temperature averages for the cooling season. The effect of the TIM-AG-PCM wall on thermal performance through TL, DF, and the total amount of heat transferred and its effect on thermal comfort through mean radiant temperature analysis were analyzed.

As a result of the study, numerical data and transient simulation data revealed that the TIM-AG-PCM wall positively affects the passive design by reducing the energy load while providing indoor comfort conditions during the heating and cooling season. The final evaluation concluded that the wall built with RT18HC and RT22HC embedded bricks in mixed order and the TIM-AG-PCM wall using

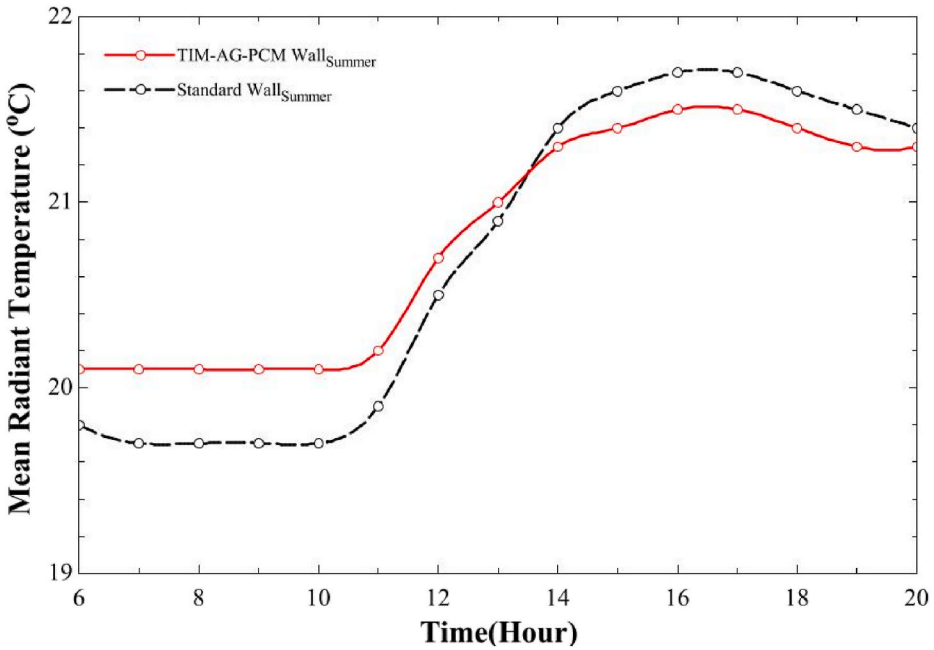


Fig. 20. MRT values of a room consisting of TIM-AG-PCM wall and standard wall installation for Ankara in the cooling season.

TIM together could be used as a building element that contributes to building energy performance in continental climate conditions. The wall with this design will significantly reduce indoor heat fluctuations and keep them at the comfort temperature level, which will increase the energy performance of the building, reduce carbon emissions, and thus reduce the environmental impact level of the buildings. In addition, by increasing the TL, decreasing the DF, and keeping the MRT temperature close to the comfort temperaturewill provide indoor comfort conditions for a long time in buildings with frequent use frequency and will make a significant contribution to passive design.

For future studies, innovative materials with different properties (insulation, energy storage) emerging as a product of developing technology can be used together to produce building elements of different qualities and constructions that will contribute to building energy performance. The most optimum building element can be developed for the continental climate region by evaluating these alternatives in terms of cost-effectiveness and building energy performance.

CRediT authorship contribution statement

Cansu Bekler: Writing – original draft, Validation, Supervision, Software, Investigation, Formal analysis. **İdil Ayçam:** Writing – review & editing, Supervision, Project administration. **Mustafa Zeki Yılmazoğlu:** Writing – original draft, Supervision, Software, Methodology, Investigation, Conceptualization.

Declaration of competing interest

The authors declare the following financial interests/personal relationships which may be considered as potential competing interests:Idil Aycam reports financial support was provided by Scientific and Technological Research Council of Turkey. If there are other authors, they declare that they have no known competing financial interests or personal relationships that could have appeared to influence the work reported in this paper.

Acknowledgement

The authors gratefully acknowledge the financial assistance of the Scientific and Technical Research Council (TUBITAK) of Türkiye provided under Project: 122M562. This publication is a part of the doctoral dissertation work by the first author in the Academic Program of Architectural, Institute of Science, Gazi University.

Appendix A. Supplementary data

Supplementary data to this article can be found online at https://doi.org/10.1016/j.jobe.2025.112058.

Data availability

Data will be made available on request.

References

[1] IEA, Global natural gas demand per sector, 2007-2025, IEA, Paris, https://www.iea.org/data-and-statistics/charts/global-natural-gas-demand-per-sector-2007-2025, Last Access Date: 10.08.2021.
[2] United Nations Environment Programme, 2020 global status report for buildings and construction: towards a zero-emission, efficient and resilient buildings and construction sector. https://globalabc.org/sites/default/files/inline-files/2020%20Buildings%20GSR_FULL%20REPORT.pdf, 2020. Last Access Date: 9.08.2021.
[3] B. Hojjati, S.H. Wade, US household energy consumption and intensity trends: a decomposition approach, Energy Policy 48 (2012) 304–314.
[4] B.P. Jelle, Traditional, state-of-the-art and future thermal building insulation materials and solutions–Properties, requirements and possibilities, Energy Build. 43 (10) (2011) 2549–2563.
[5] M. Özel, Determination of optimum insulation thickness based on cooling transmission load for building walls in a hot climate, Enerji Dönüşümü ve YöNetimi 66 (2013) 106–114, https://doi.org/10.1016/j.enconman.2012.10.002.
[6] M. Khoukhi, A. Hassan, S. Al Saadi, S. Abdelbaqi, A dynamic thermal response on thermal conductivity at different temperature and moisture levels of EPS insulation, Case Stud. Therm. Eng. 14 (2019) 100481.
[7] D. Kumar, M. Alam, P.X. Zou, J.G. Sanjayan, R.A. Memon, Comparative analysis of building insulation material properties and performance, Renew. Sustain. Energy Rev. 131 (2020) 110038, https://doi.org/10.1016/j.rser.2020.110038.
[8] X. Wang, W. Li, Z. Luo, K. Wang, S.P. Shah, A critical review on phase change materials (PCM) for sustainable and energy efficient building: design, characteristic, performance and application, Energy Build. 260 (2022) 111923, https://doi.org/10.1016/j.enbuild.2022.111923.
[9] X. Wang, L. Zhang, X. Su, H. Yang, Daylighting and energy performance of the window with transparent insulation slats in the humid subtropical climate zone, Energy Build. 300 (2023) 113685, https://doi.org/10.1016/j.enbuild.2023.113685.
[10] H. Yang, L. Zhang, X. Su, Z. Liu, Thermal performance evaluation of window with transparent insulation slats, Build. Environ. 225 (2022) 109623, https://doi.org/10.1016/j.buildenv.2022.109623.
[11] Z.L. Yang, R. Walvekar, W.P. Wong, R.K. Sharma, S. Dharaskar, M. Khalid, Advances in phase change materials, heat transfer enhancement techniques, and their applications in thermal energy storage: a comprehensive review, J. Energy Storage 87 (2024) 111329, https://doi.org/10.1016/j.est.2024.111329.
[12] S. Aghakhani, A. Ghaffarkhah, M. Arjmand, N. Karimi, M. Afrand, Phase change materials: agents towards energy performance improvement in inclined, vertical, and horizontal walls of residential buildings, J. Build. Eng. 56 (2022) 104656, https://doi.org/10.1016/j.jobe.2022.104656.

[13] Y. Chihab, R. Bouferra, A. Bouchehma, Transient thermal behavior of clay walls integrated with phase change materials, J. Energy Storage 73 (2023) 109246, https://doi.org/10.1016/j.est.2023.109246.
[14] B. Allam, T. Nehari, M.L. Benlekkam, Building brick wall thermal management optimization and temperature control based on phase change materials integration. Case study of the city of Bechar, Algeria, J. Energy Storage 73 (2023) 109043, https://doi.org/10.1016/j.est.2023.109043.
[15] A.G. Anter, A.A. Sultan, A. Hegazi, M. El Bouz, Thermal performance and energy saving using phase change materials (PCM) integrated in building walls, J. Energy Storage 67 (2023) 107568, https://doi.org/10.1016/j.est.2023.107568.
[16] Y. Zhou, J. Zhu, Y. Zhang, X. Zhou, X. Sun, Structure and regional optimization of a phase change material Trombe wall system, Energy 305 (2024) 132273, https://doi.org/10.1016/j.energy.2024.132273.
[17] M. Fan, G. Feng, L. Wang, X. Kong, H. Li, Experimental study of breathable and heterogeneous phase change material (B&H-PCM) wall for all-season thermal performance enhancement, Energy 291 (2024) 130461, https://doi.org/10.1016/j.energy.2024.130461.
[18] Y. Zhang, X. Sun, M.A. Medina, Experimental assessment of concrete masonry units integrated with insulation and phase change material: a wall-pattern study, Energy 289 (2024) 130038, https://doi.org/10.1016/j.energy.2023.130038.
[19] M. Nizovtsev, A. Sterlyagov, Effect of phase change material (PCM) on thermal inertia of walls in lightweight buildings, J. Build. Eng. 82 (2024) 107912, https://doi.org/10.1016/j.jobe.2023.107912.
[20] H.K. Jalghaf, E. Kovács, Simulation of phase change materials in building walls using effective heat capacity model by recent numerical methods, J. Energy Storage 83 (2024) 110669, https://doi.org/10.1016/j.est.2024.110669.
[21] R. Baetens, B.P. Jelle, A. Gustavsen, Phase change materials for building applications: a state-of-the-art review, Energy Build. 42 (9) (2010) 1361–1368.
[22] A.M.V.D.O. Sá, Sustentabilidade na construção: comportamento térmico de edifícios em Portugal usando materiais de mudança de fase, Universidade do Porto, Porto, 2012. Doctoral dissertation.
[23] M. Prabhakar, M. Saffari, A. de Gracia, L.F. Cabeza, Improving the energy efficiency of passive PCM system using controlled natural ventilation, Energy Build. 228 (2020) 110483.
[24] S.N. Al-Saadi, Z.J. Zhai, Modeling phase change materials embedded in building enclosure: a review, Renew. Sustain. Energy Rev. 21 (2013) 659–673.
[25] F. Kuznik, D. David, K. Johannes, J.J. Roux, A review on phase change materials integrated in building walls, Renew. Sustain. Energy Rev. 15 (1) (2011) 379–391.
[26] M. Pomianowski, P. Heiselberg, Y. Zhang, Review of thermal energy storage technologies based on PCM application in buildings, Energy Build. 67 (2013) 56–69, https://doi.org/10.1016/j.enbuild.2013.08.006.
[27] T. Yang, Y. Ding, B. Li, A.K. Athienitis, A review of climate adaptation of phase change material incorporated in building envelopes for passive energy conservation, Build. Environ. 244 (2023) 110711, https://doi.org/10.1016/j.buildenv.2023.110711.
[28] U. Stritih, P. Novak, Solar heat storage wall for building ventilation, Renew. Energy 8 (1–4) (1996) 268–271.
[29] H. Manz, P.W. Egolf, P. Suter, A. Goetzberger, TIM–PCM external wall system for solar space heating and daylighting, Sol. Energy 61 (6) (1997) 369–379.
[30] N. Kienzl, Advanced Building Skins: Translucent Thermal Storage Elements, Doctoral dissertation, Massachusetts Institute of Technology, 1999.
[31] Y. Berthou, P.H. Biwole, P. Achard, H. Sallée, M. Tantot-Neirac, F. Jay, " Full scale experimentation on a new translucent passive solar wall combining silica aerogels and phase change materials", Sol. Energy 115 (2015) 733–742.
[32] F. Souayfane, P.H. Biwole, F. Fardoun, Thermal behavior of a translucent superinsulated latent heat energy storage wall in summertime, Appl. Energy 217 (2018) 390–408.
[33] F. Souayfane, P.H. Biwole, F. Fardoun, P. Achard, Energy performance and economic analysis of a TIM-PCM wall under different climates, Energy 169 (2019) 1274–1291.
[34] D. Heim, P. Klemm, Numerical solution of TIM-PCM solar thermal storage system with ESP-r, Research Build. Phys. (2003) 683–690.
[35] D. Heim, Whole year analysis of TIM-PCM solar thermal storage Wall. Proceeding of SimBuild, 2004, pp. 1–8.
[36] P.O. Braun, A. Goetzberger, J. Schmid, W. Stahl, Transparent insulation of building facades—steps from research to commercial applications, Sol. Energy 49 (5) (1992) 413–427.
[37] J.O. Dalenbäck, Solar energy in building renovation, Energy Build. 24 (1) (1996) 39–50.
[38] A. Raicu, H.R. Wilson, P. Nitz, W. Platzer, V. Wittwer, E. Jahns, Façade systems with variable solar control using thermotropic polymer blends, Sol. Energy 72 (1) (2002) 31–42.
[39] G.M. Wallner, R.W. Lang, H. Schobermayr, H. Hegedys, R. Hausner, Development and application demonstration of a novel polymer film based transparent insulation wall heating system, Sol. Energy Mater. Sol. Cell. 84 (1–4) (2004) 441–457.
[40] G.M. Wallner, R. Hausner, H. Hegedys, H. Schobermayr, R.W. Lang, Application demonstration and performance of a cellulose triacetate polymer film based transparent insulation wall heating system, Sol. Energy 80 (11) (2006) 1410–1416.
[41] C. Li, X. Wen, W. Cai, J. Wu, J. Shao, Y. Yang, M. Wang, Energy performance of buildings with composite phase-change material wallboards in different climatic zones of China, Energy Build. 273 (2022) 112398.
[42] B. Jangeldinov, S.A. Memon, J. Kim, M. Kabdrakhmanova, Evaluating the energy efficiency of PCM-integrated lightweight steel-framed building in eight different cities of warm summer humid continental climate, Adv. Mater. Sci. Eng. 2020 (2020) 1–16.
[43] M. Sinka, D. Bajare, A. Jakovics, J. Ratnieks, S. Gendelis, J. Tihana, Experimental testing of phase change materials in a warm-summer humid continental climate, Energy Build. 195 (2019) 205–215.
[44] H. Bulut, O. Büyükalaca, T. Yılmaz, New models for simulating daily minimum, daily maximum and hourly outdoor temperatures. Proceedings of the First International Exergy, Energy and Environmeni Symposium, İzmir, Turkey, 2003, pp. 13–17.
[45] H. Bulut, O. Büyükalaca, Simple model for the generation of daily global solar-radiation data in Turkey, Uygulanan Enerji 84 (5) (2007) 477–491, https://doi.org/10.1016/j.apenergy.2006.10.003.
[46] A. Kurnuç Çırakman, Faz değiştiren madde içeren bina güney duvarının deneysel olarak incelenmesi. Doktora Tez Çalışması, Fen Bilimleri Enstitüsü, Atatürk Üniversitesi, Erzurum, 2010.
[47] C.M. Lai, C.M. Chiang, How phase change materials affect thermal performance: hollow bricks, Build. Res. Inf. 34 (2) (2006) 118–130.
[48] E. Elnajjar, Using PCM embedded in building material for thermal management: performance assessment study, Energy Build. 151 (2017) 28–34.
[49] Z. Aketouane, M. Malha, D. Bruneau, A. Bah, B. Michel, M. Asbik, O. Ansari, Energy savings potential by integrating Phase Change Material into hollow bricks: the case of Moroccan buildings, in: Building Simulation, vol. 11, Tsinghua University Press, 2018, pp. 1109–1122, 6.
[50] R. Saxena, D. Rakshit, S.C. Kaushik, Experimental assessment of Phase Change Material (PCM) embedded bricks for passive conditioning in buildings, Renew. Energy 149 (2020) 587–599.
[51] N.S. Bondareva, M.A. Sheremet, Natural convection melting influence on the thermal resistance of a brick partially filled with phase change material, Fluids 6 (7) (2021) 258.
[52] N.S. Bondareva, M. Sheikholeslami, M.A. Sheremet, The influence of external temperature and convective heat exchange with an environment on heat transfer inside phase change material embedded brick, J. Energy Storage 33 (2021) 102087.
[53] M.K. Gupta, P.K.S. Rathore, R. Kumar, N.K. Gupta, Experimental analysis of clay bricks incorporated with phase change material for enhanced thermal energy storage in buildings, J. Energy Storage 64 (2023) 107248, https://doi.org/10.1016/j.est.2023.107248.
[54] Rubitherm, PCM RT-LINE: wide-ranging organic PCM for your application. https://www.rubitherm.eu/en/index.php/productcategory/organische-pcm-rt, 2024. Last Access Date: 18.11.2024.
[55] Cabot, “LUMIRA® translucent aerogel LA1000; LA2000”. https://www.cabotcorp.com/solutions/products-plus/aerogel/particles, 2024. (Accessed 18 November 2024). Last Access Date.
[56] Climate-data, İklim Ankara. https://tr.climate-data.org/asya/tuerkiye/ankara/ankara-172/. (Accessed 14 October 2024). Last Access Date.
[57] Turkish State Meteorological, Cities & holiday resorts: ANKARA. https://www.mgm.gov.tr/eng/forecast-cities.aspx. (Accessed 14 October 2024). Last Access Date.

[58] ASHRAE Standart 55, Thermal Environment Conditions for Human Occupancy, ASHRAE, 2003.
[59] K. Bakırcı, Estimation of solar radiation by using ASHRAE clear-sky model in Erzurum, Turkey, Energy Sources, Part A 31 (3) (2009) 208–216.
[60] M. Charai, H. Sghiouri, A. Mezrhab, M. Karkri, Thermal insulation potential of non-industrial hemp (Moroccan cannabis sativa L.) fibers for green plaster-based building materials, J. Clean. Prod. 292 (2021) 126064.
[61] Y.A. Çengel, M.A. Boles, M. Kanoglu, Thermodynamics: an Engineering Approach, 5 Edition, McGraw-hill, New York, 2011, p. 445.
[62] R. Duffin, G. Knowles, Optimal thermal phase shift filters, Adv. Appl. Math. 4 (2) (1983) 197–211, https://doi.org/10.1016/0196-8858(83)90010-6.
[63] H. Asan, Y. Sancaktar, Effects of Wall's thermophysical properties on time lag and DF, Enerji ve Binalar 28 (2) (1998) 159–166, https://doi.org/10.1016/S0378-7788(98)00007-3.
[64] H. Asan, Effects of wall's insulation thickness and position on time lag and DF, Energy Build. 28 (3) (1998) 299–305, https://doi.org/10.1016/S0378-7788(98)00030-9.
[65] H. Asan, Investigation of wall's optimum insulation position from maximum time lag and minimum DF point of view, Enerji ve Binalar 32 (2) (2000) 197–203, https://doi.org/10.1016/S0378-7788(00)00044-X.
[66] A.N.S.I. Ashrae, Standard 55-2020: Thermal Environmental Conditions for Human Occupancy, American Society of Heating, Refrigerating, and Air-Conditioning Engineers, Inc., Atlanta, 2020.
[67] Y. Lu, L. Wang, J. He, R. Yang, L. Yuan, Dimensionless resolutions for heat flux DF and time lag of the wall during cyclic variations in outdoor air temperature, Case Stud. Therm. Eng. 60 (2024) 104678, https://doi.org/10.1016/j.csite.2024.104678.
[68] Y. Lu, J. Hu, J. Yu, L. Yuan, K. Bao, Analytical solutions for DF and phase shift of wall under periodic fluctuation of outdoor air temperature, Appl. Therm. Eng. 242 (2024) 122487, https://doi.org/10.1016/j.applthermaleng.2024.122487.
[69] X. Jin, X. Zhang, Y. Cao, G. Wang, Thermal performance evaluation of the wall using heat flux time lag and DF, Energy Build. 47 (2012) 369–374, https://doi.org/10.1016/j.enbuild.2011.12.010.
[70] S.K. Sah, M. Krishnan, E. Rajasekar, Correlating time lag characteristics of building envelop materials on peak energy demand during indoor climate control, Available at SSRN 4184579, 2022.
[71] F. Bilgin, M. Arici, Effect of phase change materials on time lag, DF and heat-saving, Acta Phys. Pol., A 132 (3) (2017) 1102–1105.
[72] M.A. Izquierdo-Barrientos, J.F. Belmonte, D. Rodríguez-Sánchez, A.E. Molina, J.A. Almendros-Ibáñez, A numerical study of external building walls containing phase change materials (PCM), Appl. Therm. Eng. 47 (2012) 73–85.
[73] I. Asadi, M. Hashemi, B. Sajadi, N.B. Mahyuddin, M.H. Baghban, M. Esfandiari, K. Yan, Evaluating the time lag and decrement factor of mortar and concrete containing OPBC as an agricultural by-product lightweight aggregate, Case Stud. Therm. Eng. 41 (2023) 102609.
[74] P.M. Toure, Y. Dieye, P.M. Gueye, V. Sambou, S. Bodian, S. Tiguampo, Experimental determination of time lag and decrement factor, Case Stud. Constr. Mater. 11 (2019) e00298.
[75] H. Asan, Numerical computation of time lags and DFs for different building materials, Build. Environ. 41 (5) (2006) 615–620.
[76] N. Özbalta, The effects of insulation location and thermo-physical properties of various external wall materials on DF and time lag, Sci. Res. Essays 5 (23) (2010) 3646–3659.
[77] D. Bienvenido-Huertas, J.A. Fernández Quiñones, J. Moyano, C.E. Rodríguez-Jiménez, Patents analysis of thermal bridges in slab fronts and their effect on energy demand, Energies 11 (9) (2018) 2222.
[78] L.M.F. Purwanto, Heat transfer on residential roofs with the HT-Flux software, ARTEKS: Jurnal Teknik Arsitektur 8 (3) (2023) 495–502.
[79] M.F. Alkadri, M.R.C. Agung, F. De Luca, An integrated computational method for calculating dynamic thermal bridges of building facades in tropical countries, Front. Architect. Res. 13 (1) (2024) 201–218.
[80] EN ISO 7730, Ergonomics of Thermal Environment-Analytical Determination and Interpretation of Thermal Comfort Using Calculation of the PMV and PPD Indices and Local Thermal Comfort Criteria, International Organization for Standardization, Geneva, 2005.
[81] J.F. Kreider, P.S. Curtiss, A. Rabl, Heating and Cooling of Buildings: Design for Efficiency, CRC Press, 2009.
[82] M. Arıcı, F. Bilgin, M. Krajčík, S. Nižetić, H. Karabay, Energy saving and CO2 reduction potential of external building walls containing two layers of phase change material, Energy 252 (2022) 124010.
[83] R. Courant, K. Friedrichs, H. Lewy, Über die partiellen Differenzengleichungen der mathematischen Physik, Math. Ann. 100 (1) (1928) 32–74.